

1  
2  
3  
4  
5  
6  
7  
8  
9  
10  
11  
12  
13  
14  
15  
16  
17  
18  
19  
20  
21  
22  
23  
24  
25  
26  
27  
28  
29  
30

**Morphological and transcriptomic evidence for ammonium induction of sexual reproduction in *Thalassiosira pseudonana* and other centric diatoms**

Eric R. Moore<sup>1</sup>, Briana S. Bullington<sup>1</sup>, Alexandra J. Weisberg<sup>2</sup>, Yuan Jiang<sup>3</sup>, Jeff Chang<sup>2</sup>,  
Kimberly H. Halsey<sup>1\*</sup>

<sup>1</sup>Department of Microbiology, Oregon State University, Corvallis, Oregon 97331, USA

<sup>2</sup>Department of Botany and Plant Pathology, Oregon State University, Corvallis, Oregon 97331, USA

<sup>3</sup>Department of Statistics, Oregon State University, Corvallis, Oregon 97331, USA

\* Corresponding Author: [halseyk@science.oregonstate.edu](mailto:halseyk@science.oregonstate.edu)

31 **Abstract:**

32 The reproductive strategy of diatoms includes asexual and sexual phases, but in many species,  
33 including the model centric diatom *Thalassiosira pseudonana*, sexual reproduction has never  
34 been observed. Furthermore, the environmental factors that trigger sexual reproduction in  
35 diatoms are not understood. Although genome sequences of a few diatoms are available, little is  
36 known about the molecular basis for sexual reproduction. Here we show that ammonium reliably  
37 induces the key sexual morphologies, including oogonia, auxospores, and spermatogonia, in two  
38 strains of *T. pseudonana*, *T. weissflogii*, and *Cyclotella cryptica*. RNA sequencing revealed 1,274  
39 genes whose expression patterns changed when *T. pseudonana* was induced into sexual  
40 reproduction by ammonium. Some of the induced genes are linked to meiosis or encode flagellar  
41 structures of heterokont and cryptophyte algae. The identification of ammonium as an  
42 environmental trigger suggests an unexpected link between diatom bloom dynamics and  
43 strategies for enhancing population genetic diversity.

44 **Introduction:**

45           Diatoms are protists that form massive annual spring and fall blooms in aquatic  
46 environments and are estimated to be responsible for about half of photosynthesis in the global  
47 oceans [1]. This predictable annual bloom dynamic fuels higher trophic levels and initiates  
48 delivery of carbon into the deep ocean biome. Diatoms have complex life history strategies that  
49 are presumed to have contributed to their rapid genetic diversification into ~200,000 species [2]  
50 that are distributed between the two major diatom groups: centrics and pennates [3]. A defining  
51 characteristic of all diatoms is their restrictive and bipartite silica cell wall that causes them to  
52 progressively shrink during asexual cell division. At a critically small cell size and under certain  
53 conditions, auxosporulation restitutes cell size and prevents clonal death [4-6]. The entire  
54 lifecycles of only a few diatoms have been described and rarely have sexual events been  
55 captured in the environment [7-9].

56           So far, all centric diatoms appear to share the process of oogamous sexual reproduction  
57 (Fig 1). The average cell size of a population of asexually dividing diatoms decreases as a result  
58 of differential thecae inheritance. At a critically small size, cells become eligible to differentiate  
59 into male and female cells. Meiosis in the male spermatogonangium produces multinucleate  
60 spermatogonia that divide into individual haploid spermatocytes. Meiosis in the female oogonia  
61 produces a single functional haploid nucleus that is fertilized by a flagellated spermatocyte  
62 through an opening in the oogonia thecae. Fertilized oogonia expand into a large auxospore  
63 where new, large thecae are formed for the new, enlarged initial cell. Auxosporulation can also  
64 occur asexually, but it is considered an ancillary pathway for cell size restitution in diatom  
65 species that have a sexual path for reproduction [5].

66

67           The environmental factors that trigger formation of sexual cells and sexual reproduction  
68   in centric diatoms are not well understood [10, 11], but sexualization appears to be strongly  
69   associated with conditions causing synchronous sexuality in cells experiencing growth stress  
70   [12]. Besides the size threshold requirement, previous observations indicate that sexualization is  
71   possible when active growth has ceased, causing cell cycle arrest [13, 14] and cell densities are  
72   sufficient to permit successful fertilization of the oogonia by the spermatocyte [15]. Light  
73   interruption with an extended dark period [13], changing salinities, and nutrient shifts [16], have  
74   sometimes been successful in inducing sexual reproduction, probably by causing cell cycle  
75   arrest. Recently, pheromones produced by the pennate diatom, *Seminavis robusta*, have been  
76   identified that cause cell cycle arrest and induce the sexual pathway [17]. However, we are aware  
77   of no method that reliably causes induction of all of the sexual stages of centric diatoms shown  
78   in figure 1.

79           The ecological importance of diatoms, combined with their potential uses in materials  
80   chemistry, drug delivery, biosensing [18, 19], and bioenergy [20, 21], prompted genome  
81   sequencing of *T. pseudonana* CCMP1335 (a ‘centric’ diatom collected from the North Atlantic  
82   Ocean) and *Phaeodactylum tricornutum* (a ‘pennate’ diatom), which have become model  
83   organisms for experimental studies [22, 23]. However, sexual morphologies have never been  
84   observed in either of these species or in the vast majority of diatoms [10]. The inability to  
85   reliably control the sexual cycle in centric diatoms has severely hindered studies to understand  
86   the silica deposition process, as well as the genetic regulation, ecology, and evolution of sex [10,  
87   24, 25]. Both of the model diatoms were thought to have repurposed their extant genetic toolkits  
88   and lost the need and ability for a sexual lifestyle [10, 11, 26].

89 Here we show that two strains of *T. pseudonana* and two other centric species, *T.*  
90 *weissflogii* and *Cyclotella cryptica*, can be reliably induced into the sexual reproductive pathway  
91 when cells are below the critical size threshold and exposed to ammonium during the stationary  
92 phase of growth. Ammonium induced oogonia, auxospore, and spermatocyte formation in each  
93 of these species. Induction of sexuality was further supported by RNA sequencing (RNAseq)  
94 which revealed 1,274 genes whose expression patterns changed when *T. pseudonana* became  
95 sexualized by ammonium. Meiosis genes and genes associated with flagellar structures of  
96 heterokont and cryptophyte algae were differentially expressed in ammonium-induced cells  
97 compared to nitrate grown cells. We anticipate that this discovery will open opportunities to  
98 study the evolution of diatom lifecycles and facilitate expansion of diatom breeding to explore  
99 functional genetics for molecular ecology, nanotechnology and biofuels applications.

100

## 101 **Results and Discussion:**

### 102 ***Ammonium triggers sexual morphologies***

103 We observed *T. pseudonana* CCMP1335 cell morphologies consistent with sexual  
104 reproduction when cells were propagated in artificial seawater medium supplemented with  
105 ammonium. The proportion of cells that differentiated into sexual cell types was dependent on  
106 ammonium concentration, with up to 39% of the population identified as oogonia or auxospores  
107 in cultures supplemented with 800  $\mu\text{M}$   $\text{NH}_4\text{Cl}$  (Fig 2A). Oogonia and auxospores were first  
108 observed at the onset of stationary phase and reached maximum population proportions in late  
109 stationary phase (Fig 2A). Ammonium also induced oogonia and auxospore production in *T.*  
110 *pseudonana* CCMP1015 (collected from the North Pacific Ocean), *T. weissflogii*, and *Cyclotella*  
111 *cryptica* (Fig S1). A few oogonia and auxospores were observed in nitrate grown cultures with

112 no added ammonium (Fig 2A and S1). However, with the exception of nitrate grown *C. cryptica*  
113 cultures, which generated oogonia and auxospores constituting 11% of the total population,  
114 oogonia and auxospores were only a small percentage of the total population in nitrate-grown *T.*  
115 *pseudonana* and *T. weissflogii*. Even though auxospores can have diameters 3-4 times that of  
116 asexual cells, such small population proportions do not lead to discernable shifts in cell size  
117 distributions obtained by particle size analysis (e.g., Coulter counter, a commonly used method  
118 to assess population size). We initially observed auxospores when performing visual inspections  
119 of our cultures. For the data reported here, oogonia and auxospores were quantified by manually  
120 counting the cell types using a hemocytometer. We suspect that reliance on laboratory  
121 instruments such as particle counters and flow cytometers in place of microscopic analysis is one  
122 reason that sexual morphologies in these well-studied diatom species have gone undetected until  
123 now. Laboratory stock cultures are typically maintained in media with low concentrations of  
124 nitrogen, especially when ammonium is supplied as the nitrogen source because it has been  
125 considered to be toxic to diatoms in high concentrations [27]. Therefore, it may not be surprising  
126 that sexual cells have gone un-noticed due to the low rates of sexual induction in the presence of  
127 low ammonium concentrations (Fig. 2A).

128

129       Cells differentiated into oogonia and auxospores regardless of whether ammonium was  
130 supplied at inoculation or at the onset of stationary phase (Fig. 1B). Thus, it appears that  
131 stationary phase and ammonium availability are key factors that trigger formation of sexual cells  
132 in centric diatoms. Resource depletion can arrest the cell cycle [14], and the presence of  
133 ammonium at the onset of stationary phase appears to activate the sexual cycle. Auxospore  
134 formation was observed in *Cyclotella meneghiniana* during stationary phase [28], and other

135 protists initiate sex under stress in response to nutrient depletion or oxidative DNA damage [29].  
136 Ammonium can inhibit photosynthesis [27]; however, diatoms, including *T. pseudonana*, can  
137 acclimate to millimolar ammonium concentrations [30]. It is possible that high ammonium  
138 concentrations intensify the stress condition required for the sexual pathway. Nevertheless,  
139 ammonium consistently caused formation of ten-fold more sexualized cells than the same  
140 concentrations of nitrate (Fig 2 and S1).

141 Our results showing that ammonium induced formation of sexual cells in several centric  
142 diatom species suggests that it may serve as a key environmental factor regulating the sexual  
143 lifecycle across centric diatoms. Ammonium is typically present in very low concentrations in  
144 aquatic ecosystems. However, ammonium reached 12.6 mM in a eutrophic lake where the centric  
145 diatom, *A. subarctica*, was observed undergoing sexual reproduction [8]. Clearly, ammonium  
146 was not the growth-limiting nutrient under those conditions or in our laboratory cultures (Fig 2).  
147 *Pseudo-nitzschia* auxospore formation was positively correlated with ammonium, which was  
148 measured to be 14  $\mu$ M during a major bloom event off the coast of Washington [7]. Thus, the  
149 formation of sexual cells appears to be triggered by the presence of ammonium while at least one  
150 other growth factor becomes limiting, such as light (discussed below), phosphorous, silica [7],  
151 vitamins, or trace elements.

152 Cell differentiation in *T. pseudonana* was induced irrespective of growth rate in  
153 exponential phase, light intensity, or light regime. However, the growth parameters did affect the  
154 proportion of differentiated cells. Oogonia and auxospores were only 0.5% of the population  
155 when grown under very low light (5  $\mu$ E) with 200  $\mu$ M  $\text{NH}_4\text{Cl}$  and increased to 39% when grown  
156 under moderate light (100  $\mu$ E) and 800  $\mu$ M  $\text{NH}_4\text{Cl}$  (Table 1). The proportions of oogonia and  
157 auxospores increased with light up to moderate intensities (70-100  $\mu$ E) but decreased at high

158 (220  $\mu$ E) intensities (Table 1), suggesting that photon flux has an important role in meeting the  
159 energetic demands of sexual reproduction. Other work showed sexualization was more prevalent  
160 at light <50  $\mu$ E [31] or with the addition of a dark period [13, 32, 33]. Likely, the optimum light  
161 intensity or need for a dark period to precede sexual induction [34] is species-specific and linked  
162 to adaptive life histories [5].

163

### 164 ***Visualization of sexual morphologies***

165 Confocal, light, and scanning electron microscopy were used to document the cell  
166 morphologies at various stages in the life history cycle of *T. pseudonana* (Fig 3 and S2). Oogonia  
167 were elongated relative to asexually growing vegetative cells and exhibited a bent morphology  
168 and swelling of the plasma membrane at the junction of the hypotheca and epitheca (Figs 3B, 3C  
169 and S2B-D). In oogonia, cellular contents became localized to the ends of the cell resulting in an  
170 apparent empty space near the area of membrane swelling where fertilization likely occurs [5].

171

172 *T. pseudonana* spermatogonium harbored at least eight nuclei (Fig 3D), suggesting that a  
173 depauperating mitosis preceded meiosis [11, 35]. Sperm released were very small, about 1  $\mu$ m,  
174 and flagellated (Figs 3E and S2E, S2F), but they often became entangled with other cells and  
175 debris [8, 36, 37]. Sperm cells attached to oogonia at the junction of the thecae for fertilization  
176 (Figs 3F, 3G and S2I, S2J) as shown in *T. punctigera* [38]. Also similar to *T. punctigera*, flagella  
177 were not visible at that stage, possibly because flagella are abandoned upon attachment to the  
178 oogonia [36].

179 Oogonia developed into auxospores and these conspicuous cell morphologies were  
180 always observed in cultures induced by ammonium. Auxospores were larger than vegetative



181 cells and oogonia, ranging from about 6 to 20  $\mu\text{m}$  in diameter, with most being 10-15  $\mu\text{m}$  in  
182 diameter (Figs 3H, 3I and S2G, S2H, S2L). Auxospores were spherical, with most of the cellular  
183 contents localized to one side (Fig 3H, 3I and S2G, S2H, S2L) and sometimes showing slight  
184 distention where the mother valve was shed (Fig 3I), as described in *Stephanodiscus niagarae*  
185 [39]. Thecae remained attached in some cases, especially on smaller cells. Oogonia, auxospores,  
186 and spermatogonia in the other species studied displayed similar morphologies to those observed  
187 in *T. pseudonana* and other centric diatoms (Figs 3L-O, S2M-P and 4A) [11, 16, 28, 33, 35, 37,  
188 38, 40, 41].

189

190 Changes in DNA content in *T. pseudonana* cells induced into sexuality by ammonium  
191 were observed using flow cytometry-based analysis. Fluorescence-activated cell sorting (FACS)  
192 analysis showed that as the culture progressed from exponential into stationary growth phases,  
193 the diploid population (Fig 4B) expanded to include DNA fluorescence intensities that were  
194 consistent with the presence of spermatogonangia and spermatogonia containing multiple  
195 gametes (Fig 4C). In late stationary phase, a new population was observed that had DNA  
196 fluorescence signals consistent with haploid sperm cells with little to no chlorophyll [13] (Fig  
197 4D).

198 Cell size restitution via auxosporulation produced initial cells that were considerably  
199 larger than the parent cells that were maintained in nitrate and already at or below the critical  
200 size threshold for induction into sexuality. We serially transferred ammonium-induced cultures  
201 with high proportions of auxospores to generate *T. pseudonana*, *T. weissflogii*, and *C. cryptica*  
202 cultures that were enriched in initial cells. The average cell diameters of the resulting cultures

203 were larger relative to stock cultures maintained in nitrate (Fig 4E and S3). The *T. pseudonana*  
204 initial cells were 7-12  $\mu\text{m}$ , the largest size reported for this species (Figs 3J, 3K, S2K).

205 We identified oogonia, male gametes, auxospores, and initial cells in cultures of the  
206 model centric diatom, *T. pseudonana* providing new evidence for sexuality in this species that  
207 was previously assumed to be asexual [10]. Although cell enlargement through  
208 asexual/apomictic mechanisms has been recorded in other species [42-44], the presence of all  
209 sexual cell types, and the expression of meiotic genes (discussed below), suggest apomixis is not  
210 the mechanism being used by *T. pseudonana* for cell enlargement. Furthermore, apomixis  
211 typically occurs in species that also undergo sexual reproduction [5]. Only spermatogenesis had  
212 previously been reported in *T. weissflogii* [13, 45], but we have now also documented induction  
213 of oogonia and auxospores by ammonium and subsequent formation of initial cells in this  
214 species. A major challenge in visualizing the morphological characteristics of these species is  
215 their smaller cell sizes compared to other species for which morphological details have been  
216 documented. Now that we have determined a reliable method for inducing the sexual  
217 morphologies, future studies will dissect additional details associated with the sexual pathways  
218 in these, and perhaps other species inducible by ammonium, to determine their variation from  
219 other centric diatoms. For example, the presence of auxospore scales, precise timing of  
220 fertilization and meiotic activity, repeated auxosporulation, and polyspermy events (e.g., [38]).

221

### 222 ***Gene expression analysis of ammonium induced sexual morphologies***

223 We used RNAseq to identify genes that were differentially expressed in conditions that  
224 triggered cell differentiation into sexual morphologies. We compared the transcriptomes of *T.*  
225 *pseudonana* harvested in exponential (EXP), stationary (STA), and late stationary phases (L-

226 STA). Cells were grown in 100  $\mu\text{M}$   $\text{NaNO}_3$  or, to capture a dose-dependent change in gene  
227 expression, either 100 or 800  $\mu\text{M}$   $\text{NH}_4\text{Cl}$  (Fig S4). We identified genes that were significantly  
228 differentially expressed in multiple pairwise comparisons of growth phases and nitrogen sources  
229 (Tables S1-S11). Next, we examined the statistical interactions of pairwise condition  
230 comparisons to identify genes with significantly greater or lesser magnitude changes in  
231 expression between growth stages in the presence of ammonium relative to 100  $\mu\text{M}$   $\text{NaNO}_3$  (Fig  
232 5A and S5).

233 This conservative approach yielded a total of 1,274 genes in the four analyses of  
234 statistical interactions (Supplemental Tables S12-S15). A total of 89 of the genes have an  
235 annotated function (Fig. 5A; Table S16). The set of 89 genes includes four meiotic genes (*mcm2*,  
236 *mcm8*, *mcm9*, and *mlh1*, Fig 4B and S6) that were also up-regulated in pennate diatoms during  
237 sexual reproduction [26]. The Mcm family of DNA helicases function in DNA replication, with  
238 *mcm8*, *mcm9*, and *mlh1*, having roles in double stranded break repair [46-48]. Mcm8 was one of  
239 the four genes related to meiosis that were upregulated in the pennate diatom, *Seminavis robusta*  
240 during treatment with a sex-inducing pheromone [17]. Eight genes in our list are homologous to  
241 yeast genes involved in meiosis [49] (Fig 4B, Table S17), including genes that regulate the  
242 meiotic anaphase promoting complex (*cdc16*, *cdc23*, *ama1*) [50, 51] and *rad54*, a motor protein  
243 that regulates branch migration of Holliday junctions during homologous recombination [52].  
244 Expression of genes encoding other RAD proteins (*rad50* and *rad 51*) increased in pennate  
245 diatoms induced into meiosis [17, 26].

246 Of three ‘sexually induced genes’ that were up-regulated in *T. weissflogii* at the initiation  
247 of gametogenesis [45] and associated with sperm flagella mastigonemes [53], one, *sig3*, was  
248 significantly up-regulated in stationary phase compared to exponential phase (Fig 4B). In

249 addition, a gene encoding an intraflagellar transport protein (IFT88) was also up-regulated in  
250 ammonium induced cells during stationary phase (Fig. 4B). An IFT system is required for  
251 flagellar assembly [54] and five genes encoding IFT particle proteins, including IFT88, and a  
252 kinesin-associated protein involved in anterograde transport were found in the *T. pseudonana*  
253 genome [55]. The genes encoding Sig3 and IFT88 are unique to flagellar structures, and their  
254 differential expression in ammonium induced *T. pseudonana* compared to the nitrate-grown  
255 control treatments provide additional evidence that ammonium induced spermatogenesis in this  
256 species.

257 The MYB factor and bZIP families of proteins are transcriptional regulators that control a  
258 variety of cell processes including stress responses, development, and differentiation in plants  
259 [56]. Expression of two genes having the characteristic R2R3 MYB DNA binding domains  
260 common in plants, *myb24* and *myb16*, was generally lower in ammonium induced cultures  
261 compared to the nitrate grown controls (Fig 4B). In *Arabidopsis thaliana*, hormonal activation of  
262 *myb24* is required for stamen development and male fertility [57]. Whether *myb24*, *myb16*, and  
263 *bzip2* play roles in regulating gamete development or sex differentiation in diatoms remains to be  
264 determined.

265 The 1,274 genes provide new avenues to understand the evolution of sexuality in the  
266 Heterokont eukaryotic lineage. Diatoms emerged ~ 200 Mya, about 800 My after a eukaryotic  
267 heterotroph engulfed a red alga in the secondary endosymbiosis event that gave rise to the SAR  
268 eukaryotic supergroup [58]. Of 171 diatom genes of red algal origin [58], 17 were identified as  
269 differentially expressed in conditions that induced sexual reproduction (Table S18). None of  
270 these genes are annotated in the *T. pseudonana* genome, but in red algae they are predicted to  
271 function in transport and plastid-targeted processes [23].

272 **Conclusions:**

273           That some of the most well studied centric diatoms were never observed undergoing  
274 sexual reproduction was a mystery. Possibly even more elusive was the ability to reliably control  
275 or induce the sexual pathway of centric diatoms in the laboratory [10] despite a myriad of efforts  
276 that ranged from sweet-talk to torture. Factors that have limited progress in this field center on  
277 the problem that even under ‘favorable environmental conditions’ that result in the sexual  
278 lifecycle, only a fraction of cells undergo sexual reproduction (Fig 2). Thus, capturing the sexual  
279 event requires near constant visual observation because (a) only cells that have become  
280 sufficiently small and reach the critical size threshold can undergo sexual reproduction [59], (b)  
281 only a fraction of those size-eligible cells may undergo sexual reproduction [8, 15, 16, 31], (c)  
282 there has been a lack of understanding about what constitutes conditions that are ‘favorable’ for  
283 triggering diatom sex [5, 7], and (d) morphological changes indicative of sex may not be  
284 recognized by untrained scientists [60].

285           Our results provide strong evidence that *T. pseudonana* is a sexual organism, expressing  
286 the major morphologies associated with the sexual pathway that result in enlarged initial cells.  
287 Furthermore, the sexual pathway was reliably induced in *T. pseudonana*, and two other centric  
288 diatom species by exposure of size-eligible cells to ammonium. Ammonium triggered formation  
289 of sexual cells in a dose-dependent manner and significant changes in expression of genes  
290 involved in meiosis, spermatocyte flagellar structures and assembly, and sex differentiation.  
291 RNAseq analysis revealed many more genes with unknown functions that were expressed under  
292 conditions of sexual differentiation. Other genes involved in sex are likely to have been missed  
293 by our analysis because their changes in expression were masked by the mixed population of  
294 asexual and sexual cells, or they were not captured in the coarse time-resolution of sampling

295 used in this study. Nevertheless, our discoveries resolve two persistent mysteries that have  
296 plagued diatom researchers. Furthermore, the RNAseq data provide a subset of genes that can be  
297 used to study the molecular ecology of diatoms.

298         The ecology of centric diatom sexual reproduction that can be inferred from our findings  
299 appears best described as synchronous sexuality [12] triggered by ammonium in cells  
300 experiencing growth stress. Asexual cell cycle arrest appears to be prerequisite to activation of  
301 the diatom sexual life cycle [13, 14, 28, 29]. In the environment, diatoms bloom following  
302 elevated nutrient concentrations driven by vertical mixing, coastal upwelling, or river inputs and  
303 the bloom reaches its peak biomass when essential nutrients are depleted. Within a week, the  
304 bulk of a bloom can be consumed by heterotrophic protists [61] that excrete ammonium to  
305 maintain homeostatic elemental composition [62]. We propose that ammonium released by  
306 grazers at bloom climax may be a principal ecological trigger for sexual morphologies in centric  
307 diatoms. Synchronization of sexuality at the onset of resource depletion (stationary phase)  
308 increases the chances for successful fertilization because cell density is at its maximum [12].  
309 Environmental concentrations of ammonium in the environment rarely reach the concentrations  
310 used in this study to demonstrate the dose response effect on sexuality. Other methods that have  
311 sometimes successfully triggered sexual reproduction in other species are similarly unusual  
312 compared to environmental conditions. For example, the magnitude of the salinity shifts used to  
313 induce sexual reproduction in *Skeletonema marioni* in the laboratory do not occur in the Baltic  
314 sea [16]. Nevertheless, pulses of ammonium, shifts in salinity, and other environmental  
315 fluctuations do occur in aquatic ecosystems, and provided the other conditions for sexuality are  
316 met (e.g., cell size threshold, stress, population density), are likely to induce sexuality in at least  
317 a small fraction of a population. The presence of ammonium and the onset of stationary phase

318 also point to involvement of another growth factor whose depletion triggers sexual reproduction.  
319 The specific collection of factors that lead to sexual reproduction in diatoms in the environment  
320 is not yet known and neither is whether ammonium is a direct or indirect trigger of sexuality [4].  
321 Nevertheless, this work suggests an intriguing ecological role for ammonium in the mechanisms  
322 underlying sexuality in centric diatoms and will certainly be a valuable tool to control sexuality  
323 in the laboratory.

324 The identification of ammonium as a reliable inducer of sexuality in *T. pseudonana* and  
325 other centric diatoms has the potential to shift perspectives on diatom ecology, open avenues for  
326 the experimental investigation of diatom reproductive mechanisms, and provide tools for genetic  
327 manipulation of centric diatoms that have not heretofore been available. Diatom blooms have a  
328 global impact but the factors that control these blooms and their demise are complex and a  
329 consensus has not been reached about these processes. Our evidence suggests that induction of  
330 sexuality may play a vital role in diatom bloom conclusion and the production of genetic  
331 diversity that seeds future blooms [63]. Our analysis suggests an involvement of genes of red-  
332 algal origin, providing new lines of evolutionary enquiry. Interest in diatoms for biotechnological  
333 applications is high due to their uses in biofuels, materials chemistry and medicine. Our work  
334 will likely propel this exploration by enabling improved breeding and genetic modification to  
335 control and understand unique diatom traits.

336

### 337 **Methods**

338 Stock cultures of *T. pseudonana* (CCMP1335) were maintained in f/2 medium [64] with  
339 200  $\mu\text{M}$   $\text{NaNO}_3$  under continuous sub-saturating light at 18°C. Sexual cells were quantified in  
340 triplicate cultures of *T. pseudonana* (CCMP1335 and CCMP1015), *T. weissflogii* (CCMP1336)

341 and *C. cryptica* (CCMP332) (all obtained from NCMA) grown in f/2 amended with NaNO<sub>3</sub> or  
342 NH<sub>4</sub>Cl and grown at 18°C under 50 µE continuous light, or under variable light intensities/cycles  
343 as shown in Table 1. Cell populations were quantified using a Coulter counter (Beckman-  
344 Coulter, Indianapolis, Indiana). Oogonia and auxospores were counted using a hemocytometer.

345 We found that a modified f/2 medium yielded better cell images using light and confocal  
346 microscopy. This medium contained 0.939 mM KCl, 0.802 mM NO<sub>3</sub><sup>-</sup>, 1 mM NH<sub>4</sub>Cl, 0.05 mM  
347 glycine, 0.01 mM methionine, 0.078 mM pyruvate, 0.84 µM pantothenate, 0.985 µM 4-amino-5-  
348 hydroxymethyl-2-methylpyrimidine, 0.3 µM thiamine, 0.002 µM biotin, 0.117 µM FeCl<sub>3</sub>\*6H<sub>2</sub>O,  
349 0.009 µM MnCl<sub>2</sub>\*4H<sub>2</sub>O, 0.0008 µM ZnSO<sub>4</sub>\*7H<sub>2</sub>O, 0.0005 µM CoCl<sub>2</sub>\*6H<sub>2</sub>O, 0.0003 µM  
350 Na<sub>2</sub>MoO<sub>4</sub>\*2H<sub>2</sub>O, 0.001 µM Na<sub>2</sub>SeO<sub>3</sub>, and 0.001 µM NiCl<sub>2</sub>\*6H<sub>2</sub>O, and sparged with filter-  
351 sterilized carbon dioxide and air for 8 hours and overnight respectively. To view DNA, 1 ml live  
352 samples were stained with 5 µl 1.62 µM Hoescht 33342 (0.2 µm filtered) for 10 min. For  
353 scanning electron microscopy (SEM), 1 ml samples were diluted 1:3 with sterile f/2 and syringe  
354 filtered onto 13 mm 0.2 µm polycarbonate filters using a Swinnex filter unit. The filter was  
355 washed with 4 ml f/2 containing 0.5% gluteraldehyde and left submerged for at least 24 hours,  
356 followed by a series of 4 ml washes: 0.2 µm filtered 80%, 60%, 40%, 20% and 0% f/2, followed  
357 by 20%, 40%, 60% 80% and 100% ethanol, before critical point drying. SEM imaging was done  
358 at the Oregon State University Electron Microscope facility.

359 For flow cytometry 1 ml culture samples were fixed with 1 µl gluteraldehyde (50%) and  
360 stained with 10 µl Sybr green mix (1:25 dilution Sybr green in 0.01M Tris-EDTA, pH 8.0) for 30  
361 min. Samples were run on a FACScan flow cytometer (Becton Dickinson, Franklin Lakes, New  
362 Jersey). Settings were FL1=582 and FL3=450 for unstained cells and FL1=450 and FL3=450 for  
363 stained cells.



364 For RNAseq analysis,  $1.61 \times 10^8 - 1.10 \times 10^9$  cells from triplicate independent cultures  
365 were filtered onto 0.8  $\mu\text{m}$  47 mm polycarbonate filters during exponential, stationary and late  
366 stationary phases and flash frozen in liquid nitrogen. RNA was extracted using a Qiagen RNeasy  
367 midi kit according to modified manufacturer's instructions [65]. Silica beads (0.5 mm) were  
368 added to the cells and lysis buffer and vortexed until homogeneous before being filtered through  
369 Qias shredder columns to remove large particles. Eluted RNA was subjected to off column RNase  
370 free DNase I treatment and secondary purification according to manufacturer's  
371 recommendations. Total RNA was prepared and sequenced as a 150 bp single end library on an  
372 Illumina HiSeq 3000 at the Center for Genome Research and Biocomputing at Oregon State  
373 University. Sequencing data/interaction analyses were conducted using the Ballgown pipeline  
374 [66]. Sequencing reads were trimmed to remove sequencing adapters using BBDuk v. with the  
375 parameters "ktrim=r k=23 mink=9 hdist=1 minlength=100 tpe tbo" [67]. Reads aligned to the *T.*  
376 *pseudonana* reference genome (NCBI accession GCA\_000149405.2) using HISAT2 v. 2.0.4  
377 with the parameters " --min-intronlen 20 --max-intronlen 1500 --rna-strandness F --dta-cufflinks"  
378 [68]. Transcripts were assembled for each dataset and merged using Stringtie v 1.2.4 [69].  
379 Pairwise differential expression analyses for genes were performed using the "stattest" function  
380 in Ballgown version 2.2.0 [70]. Interaction effects were tested by comparing the models with  
381 (timepoint + treatment + timepoint \* treatment) and without (timepoint + treatment) the  
382 interaction term using the custom model option in the "stattest" function.

383 For construction of the phylogenetic tree, 18s rRNA sequences were obtained from the  
384 Silva database and aligned using Muscle v3.8.31 (default settings) [71]. A genome editor  
385 (BioEdit) was used to manually trim off overhanging sequence. The tree was built using  
386 RAxML-HPC v8.0.26 using the GTRCAT model, "-f a" option, and 1000 bootstrap replicates

387 [72]. A visual representation was created using the TreeDyn [73] tool through LIRMM  
388 (phylogeny.fr) [74].

389

390 **Acknowledgements:** The authors thank Kelsey McBeain for assistance with confocal  
391 microscopy imaging and the Electron Microscope Facility at Oregon State University for  
392 scanning electron micrographs.

393

## REFERENCES:

1. Nelson DM, Tréguer P, Brzezinski MA, Leynaert A, Quéguiner B. Production and dissolution of biogenic silica in the ocean: Revised global estimates, comparison with regional data and relationship to biogenic sedimentation *Biogeochem Cycles*. 1995;9(3):359-72.
2. Mann DG. The species concept in diatoms. *Phycologia*. 1999;38:437-95.
3. Simonsen R. The diatom system: Ideas on phylogeny. *Bacillaria*. 1979;2:9-71.
4. Lewis WM. The diatom sex clock and its evolutionary importance. *Amer Naturalist*. 1984;123:73-80.
5. Chepurnov VA, Mann DG, Sabbe K, Vyverman W. Experimental studies on sexual reproduction in diatoms. In: Jeon KW, editor. *A Survey of Cell Biology*. International Review of Cytology. 237. London, UK: Elsevier Academic Press; 2004. p. 91-154.
6. Drebes. Sexuality. In: Werner D, editor. *The Biology of Diatoms*. Botanical Monographs. 13. Oxford: Blackwell Scientific Publications; 1977. p. 250-83.
7. Holtermann KE, Bates SS, Trainer VL, Odell A, Armbrust EV. Mass sexual reproduction in the toxigenic diatoms *Pseudo-Nitzsca australis* and *P. pungens* (Bacillariophyceae) on the Washington coast, USA. *J Phycol*. 2010;46:41-52.
8. Jewson DH. Size reduction, reproductive strategy and the life cycle of a centric diatom. *Philos T R Soc B*. 1992;336:191-213.
9. Koester JA, Brawley SH, Karp-Boss L, Mann DG. Sexual reproduction in the marine centric diatom *Ditylum brightwellii* (Bacillariophyta). *Eur J Phycol*. 2008;42(4):351-66.
10. Chepurnov VA, Mann DG, von Dassow P, Vanormelingen P, Gillard J, Inze D, et al. In search of new tractable diatoms for experimental biology. *BioEssays*. 2008;30:692-702.

11. Von Dassow P, Montresor M. Unveiling the mysteries of phytoplankton life cycles: patterns and opportunities behind complexity. *J Plankton Res.* 2011;33(1):3-12.
12. Edlund MB, Stoermer EF. Ecological, evolutionary, and systematic significance of diatom life histories. *J Phycol.* 1997;33:897-918.
13. Armbrust EV, Chisholm SW, Olson RJ. Role of light and the cell cycle on the induction of spermatogenesis in a centric diatom. *J Phycol.* 1990;26(3):470-8.
14. Huysman MJJ, Vyverman W, De Veylder L. Molecular regulation of the diatom cell cycle. *J Exp Bot.* 2014;65(10):2573-84.
15. Assmy P, Henjes J, Smetacek V, Montresor M. Auxospore formation in the silica-sinking oceanic diatom *Fragilariopsis kerguelensis* (Bacillariophyceae). *J Phycol.* 2006;42:1002-6.
16. Godhe A, Kremp A, Montresor M. Genetic and microscopic evidence for sexual reproduction in the centric diatom *Skeletonema marinoi*. *Protist.* 2014;165(4):401-16.
17. Moeys S, Frenkel J, Lembke C, Gillard JTF, Devos V, Van den Berge K, et al. A sex-inducing pheromone triggers cell cycle arrest and mate attraction in the diatom *Seminavis robusta*. *Sci Reports.* 2016;6:19252.
18. Ezzati J, Dolatabadi N, de la Guardia M. Applications of diatoms and silica nanotechnology in biosensing, drug and gene delivery, and formation of complex metal nanostructures. *J Analyt Chem.* 2011;30(9):1538-48.
19. Kroth P. Molecular biology and the biotechnological potential of diatoms. *Adv Exp Med Biol.* 2007;616:23-33.
20. d'Ippolito G, Sardo A, Paris D, Vella FM, Adelfi MG, Botte P, et al. Potential of lipid metabolism in marine diatoms for biofuel production. *Biotechnology for Biofuels.* 2015;8:28-38.

21. Hildebrand D, Smith SR, Traller JC, Abbriano RM. The place of diatoms in the biofuels industry. *Biofuels*. 2012;3(2):221-40.
22. Armbrust EV, Berges JA, Bowler C, Green BR, Martinez D, Putnam NH, et al. The genome of the diatom *Thalassiosira pseudonana*: Ecology, evolution, and metabolism. *Science*. 2004;306:79-86.
23. Bowler CB, Allen AE, Badger JH, Grimwood J, Jabbari K, Kuo A, et al. The *Phaeodactylum* genome reveals the evolutionary history of diatom genomes. *Nature*. 2008;456(7219):239-44.
24. Chepurnov VA, Chaerle P, Roef L, Van Meirhaeghe A, Vanhoutte K. Classical breeding in diatoms: Scientific background and practical perspectives. *Diatom Biology. Cellular Origin, Life in Extreme Habitats and Astrobiology*. 19: Springer; 2011. p. 167-94.
25. Apt KE, Kroth-Pancic PG, Grossman A. Stable nuclear transformation of the diatom *Phaeodactylum tricornutum*. *Mol Gen Genet*. 1996;252(5):572-9.
26. Patil S, Moeys S, Von Dassow P, Huysman MJJ, Mapleson D, De Veylder L, et al. Identification of the meiotic toolkit in diatoms and exploration of meiosis-specific *SPO11* and *RAD51* homologs in the sexual species *Pseudo-nitzschia multistriata* and *Seminavis robusta*. *BMC Genomics*. 2015;2015(930).
27. Yoshiyama K, Sharp JH. Phytoplankton response to nutrient enrichment in an urbanized estuary: Apparent inhibition of primary production by overeutrophication. *Limnol Oceanogr*. 2006;51(1, part 2):424-34.
28. Hoops HJ, Floyd GL. Ultrastructure of the centric diatom, *Cyclotella meneghiniana*: vegetative cell and auxospore development. *Phycologia*. 1979;18:424-35.
29. Bernstein H, Bernstein C. Evolutionary origin of recombination during meiosis. *BioScience*. 2010;60(7):498-505.

30. Collos Y, Harrison PJ. Acclimation and toxicity of high ammonium concentrations to unicellular algae. *Mar Poll Bull.* 2014;80(1-2):8-23.
31. Mouget J-L, Gastineau R, Davidovich O, Gaudin P, Davidovich NA. Light is a key factor in triggering sexual reproduction in the pennate diatom *Haslea ostrearia*. *FEMS Microbiol Ecol.* 2009;69(2):194-201.
32. Vaultot D, Chisholm SW. A simple model for the growth of phytoplankton populations in light/dark cycles. *J Plankton Res.* 1987;9:345-66.
33. Mills KE, Kaczmarska I. Autogamic reproductive behavior and sex cell structure in *Thalassiosira angulata* (Bacillariophyta). *Botanica Mar.* 2006;49:417-30.
34. Gillard J, Devos V, Huysman MJJ, De Veylder L, D'Hondt S, Martens C, et al. Physiological and transcriptomic evidence for a close coupling between chloroplast ontogeny and cell cycle progression in the pennate diatom *Seminavis robusta*. *Plant Physiol.* 2008;148:1394-411.
35. Kaczmarska I, Pouličková A, Sato S, Edlund MB, Idei M, Watanabe T, et al. Proposals for a terminology for diatom sexual reproduction, auxospores and resting stages. *J Diatom Res.* 2013;28(3):263-94.
36. French III FW, Hargraves PE. Spore formation in the life cycles of the diatoms *Chaetoceros diadema* and *Leptocylindrus danicus*. *J Phycol.* 1985;21:477-83.
37. Idei M, Osada K, Sato S, Toyoda K, Nagumo T, Mann DG. Gametogenesis and auxospore development in *Actinocyclus* (Bacillariophyta). *PLOS One.* 2012;7(8):e41890.
38. Chepurnov VA, Mann DG, Von Dassow P, Armbrust EV, Sabbe K, Dasseville R, et al. Oogamous reproduction, with two-step auxosporulation, in the centric diatom *Thalassiosira punctigera* (Bacillariophyta). *J Phycol.* 2006;42:845-58.

39. Edlund MB, Stoermer EF. Sexual reproduction in *Stephanodiscus niagarae* (Bacillariophyta). J Phycol. 1991;27:780-93.
40. Idei M, Sato S, Nagasato C, Motomura T, Toyoda K, Nagumo T, et al. Spermatogenesis and auxospore structure in the multipolar centric diatom *Hydrosera*. J Phycol. 2015;51(1):144-58.
41. Shirokawa Y, Shimada M. Sex allocation pattern of the diatom *Cyclotella meneghiniana*. Proceedings of the Royal Society B: Biological Sciences. 2013;280(1761):20130503.
42. Nagai S, Hori Y, Manabe T, Imai I. Restoration of cell size by vegetative cell enlargement in *Coscinodiscus wailesii* (Bacillariophyceae). Phycologia. 1995;34(6):533-5.
43. Sabbe K. Apomixis in *Achnanthes* (Bacillariophyceae); development of a model system for diatom reproductive biology. Eur J Phycol. 2004;39:327-41.
44. Gallagher JC. Cell Enlargement in *Skeletonema costatum* (Bacillariophyceae). J Phycol. 1983;19:539-42.
45. Armbrust EV. Identification of a new gene family expressed during the onset of sexual reproduction in the centric diatom *Thalassiosira weissflogii*. Appl Environ Microbiol. 1999;65:3121-8.
46. Lutzmann M, Grey C, Traver S, Ganier O, Maya-Mendoza A, Ranisavljevic N, et al. MCM8- and MCM9-deficient mice reveal gametogenesis defects and genome instability due to impaired homologous recombination. Mol Cell. 2012;47(4):523-34.
47. Park J, Long DT, Lee KY, Abbas T, Shibata E, Negishi M, et al. The MCM8-MCM9 complex promotes RAD51 recruitment at DNA damage sites to facilitate homologous recombination. Mol Cell Biol. 2013;33(8):1632-44.
48. Baker SM, Plug AW, Prolla TA, Bronner CE, Harris AC, Yao X, et al. Involvement of mouse Mlh1 in DNA mismatch repair and meiotic crossing over. Nat Genet. 1996;13(3):336-42.

49. Butler G, Rasmussen MD, Lin MF, Santos MAS, Sakthikumar S, Munro CA, et al. Evolution of pathogenicity and sexual reproduction in eight *Candida* genomes. *Nature*. 2009;459:657-62.
50. Cooper KF, Mallory JJ, Egeland DB, Jarnik M, Strich R. Ama1p is a meiosis-specific regulator of the anaphase promoting complex/cyclosome in yeast. *PNAS*. 2000;97(26):14548-53.
51. Zachariae W, Shevchenko A, Andrews PD, Ciosk R, Galova M, Stark MJR, et al. Mass spectrometric analysis of the anaphase-promoting complex from yeast: Identification of a subunit related to cullins. *Science*. 1998;279(5354):1216-9.
52. Mazin AV, Mazina OM, Bugreev DV, Rossi MJ. Rad54, the motor of homologous recombination. *DNA Repair*. 2010;9(3):286-302.
53. Honda D, Shono T, Kimura K, Fujita S, Iseki M, Makino Y, et al. Homologs of the sexually induced gene 1 (*sig1*) product constitute the Stramenopile mastigonemes. *Protist*. 2007;158(1):77-88.
54. Rosenbaum JL, Witman GB. Intraflagellar transport. *Nat Rev Mol Cell Biol*. 2002;3:813-25.
55. Merchant SS, Prochnik SE, Vallon O, Harris EH, Karpowicz SJ, Witman GB, et al. The *Chlamydomonas* genome reveals the evolution of key animal and plant functions. *Science*. 2007;318(5848):245-50. doi: 10.1126/science.1143609.
56. Ambawat S, Sharma P, Yadav NR, Yadav RC. MYB transcription factor genes as regulators for plant responses: an overview. *Physiol Mol Biol Plants*. 2013;19(3):307-21.
57. Cheng H, Song S, Xiao LX, Soo HM, cheng Z, Xie D, et al. Gibberellin acts through jasmonate to control the expression of *MYB21*, *MYB24*, and *MYB57* to promote stamen filament growth in *Arabidopsis*. *Plos Genet*. 2009;5. doi: 10.1371/journal.pgen.1000440.
58. Archibald JM. The puzzle of plastid evolution. *Curr Biol*. 2009;19(2):R81-R8.
59. Geitler L. Der Formwechsel der pennaten Diatomeen. *Arch Protistenk*. 1932;78(1):1-226.

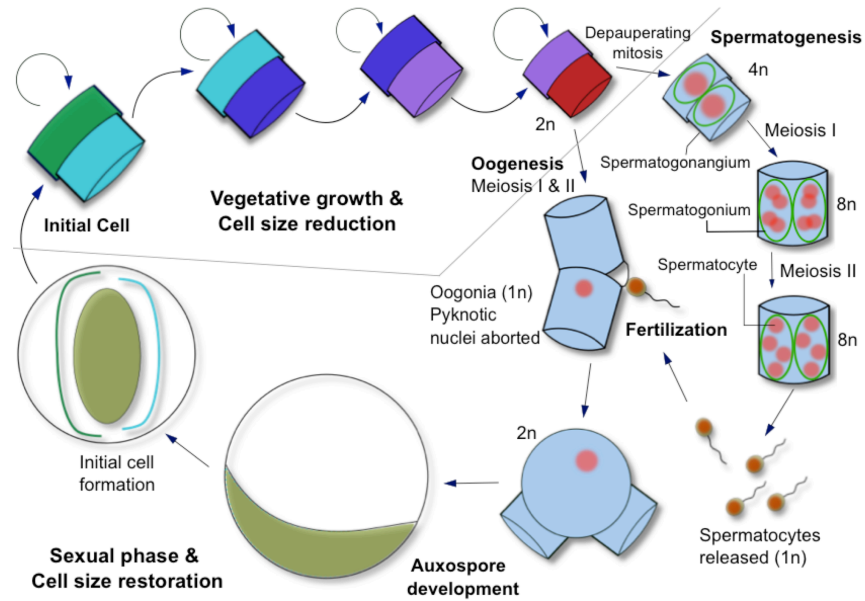


60. Mann DG. Why didn't Lund see sex in *Asterionella*? A discussion of the diatom life cycle in nature. In: Round FE, editor. *Algae and the Aquatic Environment, contributions in honour of JWG Lund*. Bristol: Biopress; 1988. p. 384-412.
61. Tillmann U. Interactions between planktonic microalgae and protozoan grazers. *J Euk Microbiol*. 2004;51:156-68.
62. Sterner RW, Elser JJ. *Ecological stoichiometry: the biology of elements from molecules to the biosphere*. Princeton, New Jersey, USA: Princeton University Press; 2002.
63. Chen G, Rynearson TA. Genetically distinct populations of a diatom co-exist during the North Atlantic spring bloom. *Limnol Oceanogr*. 2016;61(6):2165-79.
64. Guillard RRL. Culture of phytoplankton for feeding marine invertebrates. In: Smith WL, Chanley MH, editors. *Culture of Marine Invertebrate Animals*. New York: Plenum Press; 1975. p. 26-60.
65. Dyhrman ST, Jenkins BD, Rynearson TA, Saito MA, Mercier ML, Alexander H, et al. The transcriptome and proteome of the diatom *Thalassiosira pseudonana* reveal a diverse phosphorus stress response. *PLOS One*. 2012;7(3):e33768.
66. Perteau M, Kim D, Perteau GM, Leek JT, Salzberg SL. Transcript-level expression analysis of RNA-seq experiments with HISAT, StringTie and Ballgown. *Nat Prot*. 2016;11:1650-67.
67. Bushnell B. *BBtools* 2016.
68. Kim D, Langmead B, Salzberg SL. HISAT: a fast spliced aligner with low memory requirements. *Nat Methods*. 2015;12:357-60.
69. Perteau M, Perteau GM, Antonescu CM, Chang TC, Mendell JT, Salzberg SL. StringTie enables improved reconstruction of a transcriptome from RNA-seq reads. *Nat Biotech*. 2015;33(290-295):290-5.

70. Frazee AC, Perteu GM, Jaffe AE, Langmead B, Salzberg SL, Leek JT. Ballgown bridges the gap between transcriptome assembly and expression analysis. *Nat Biotech.* 2015;33(3):243-6.
71. Edgar RC. MUSCLE: a multiple sequence alignment method with reduced time and space complexity. *BMC Bioinformatics.* 2004;19(5):113.
72. Stamatakis A. RAxML-VI-HPC: maximum likelihood-based phylogenetic analyses with thousands of taxa and mixed models. *Bioinformatics.* 2006;22:2688-90.
73. Chevenet F, Brun C, Bañuls AL, Jacq B, Christen R. TreeDyn: towards dynamic graphics and annotations for analyses of trees. *BMC Bioinformatics.* 2006;7:439.
74. Dereeper A, Guignon V, Blanc G, Audic S, Buffet S, Chevenet F, et al. Phylogeny.fr: robust phylogenetic analysis for the non-specialist. *Nucleic Acids Res.* 2008;1(36):W465-W9.

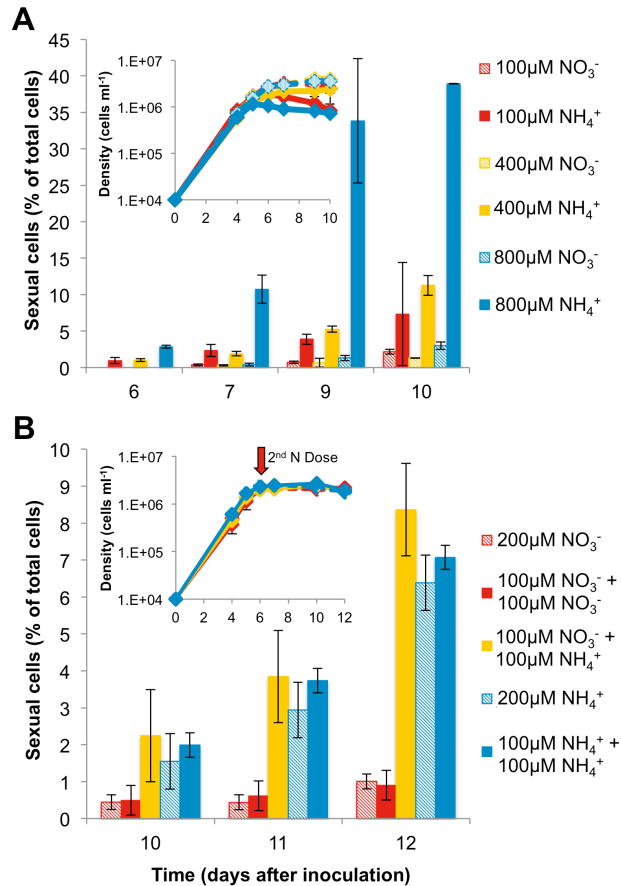
**Table 1.** Effects of growth parameters on induction of sexual reproduction in *T. pseudonana* CCMP1335, *T. weissflogii* and *C. cryptica*. Oogonia and auxospores always appeared in stationary phase. The percentage of the total population (at least 300 cells counted per replicate) differentiated into oogonia or auxospores when grown in nitrate or ammonium is shown for the day they were at their maximum number; data are mean values  $\pm$  s.d., biological replicates n=3.

Species	Light intensity ( $\mu\text{E}$ )	Light regime	Nitrogen concentration ( $\mu\text{M}$ )	Specific growth rate ( $\text{d}^{-1}$ )	Oogonia and auxospores in $\text{NO}_3^-$ (%)	Oogonia and auxospores in $\text{NH}_4^+$ (%)
<i>T. pseudonana</i>	5	24 h	200	0.28	$0.21 \pm 0.22$	$0.52 \pm 0.52$
	50	24 h	200	0.89	$3.67 \pm 0.55$	$7.67 \pm 0.50$
	50	12 h/12 h L/D	200	0.80	$0.67 \pm 0.27$	$2.32 \pm 0.52$
	220	24 h	200	1.2	$0.26 \pm 0.26$	$1.30 \pm 0.91$
	70	24 h	800	0.98	$3.01 \pm 0.52$	$38.9 \pm 0.04$
<i>C. cryptica</i>	100	24 h	800	0.38	$11.1 \pm 2.27$	$37.6 \pm 3.71$
<i>T. weissflogii</i>	100	24 h	800	0.52	$4.50 \pm 2.36$	$39.8 \pm 5.65$

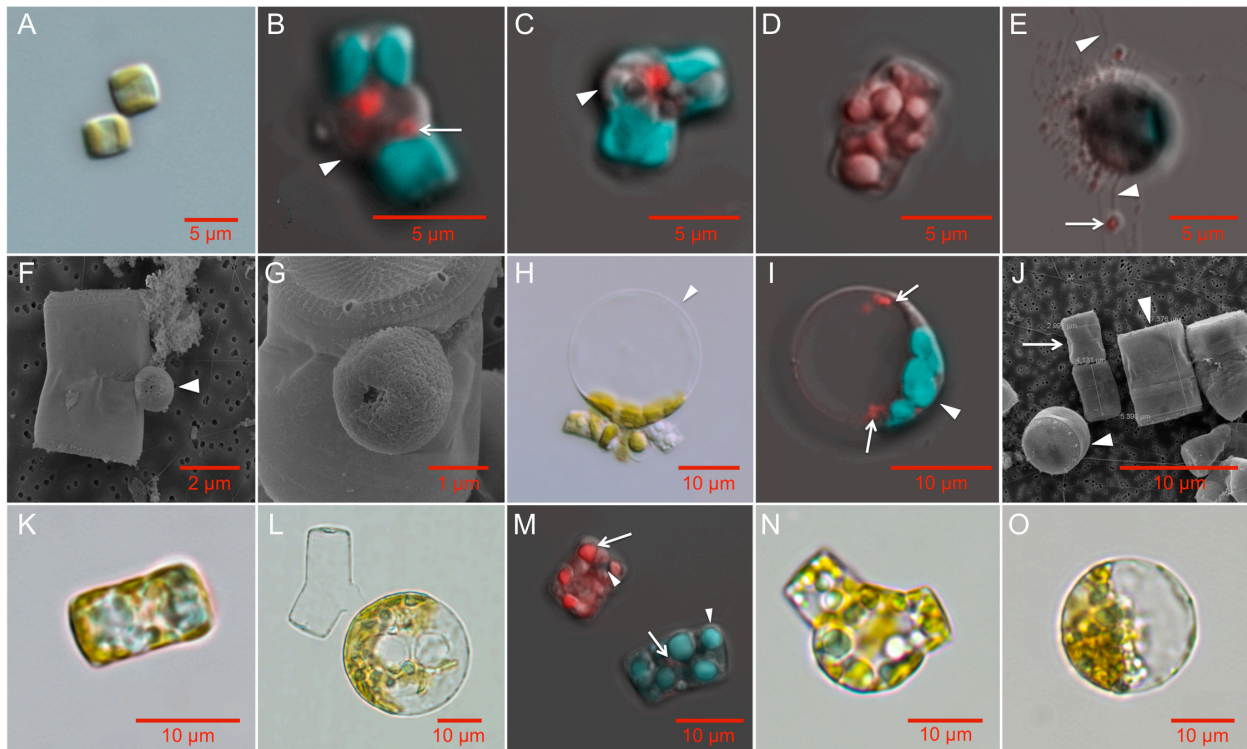


1  
2  
3  
4  
5  
6  
7  
8  
9  
10  
11

**Fig 1. The life cycle of a centric diatom.** The average cell size of a population of asexually dividing diatoms decreases as a result of differential thecae inheritance. At a critically small size, cells can initiate sexual reproduction and differentiate into male and female cells. Meiosis in the male spermatogonangium produces multinucleate spermatogonia that divide into individual haploid spermatocytes. Meiosis in the female oogonia produces a single functional haploid nucleus that is fertilized by a flagellated spermatocyte through an opening in the oogonia thecae. Fertilized oogonia expand into a large auxospore where new, large thecae are formed for the new initial cell.

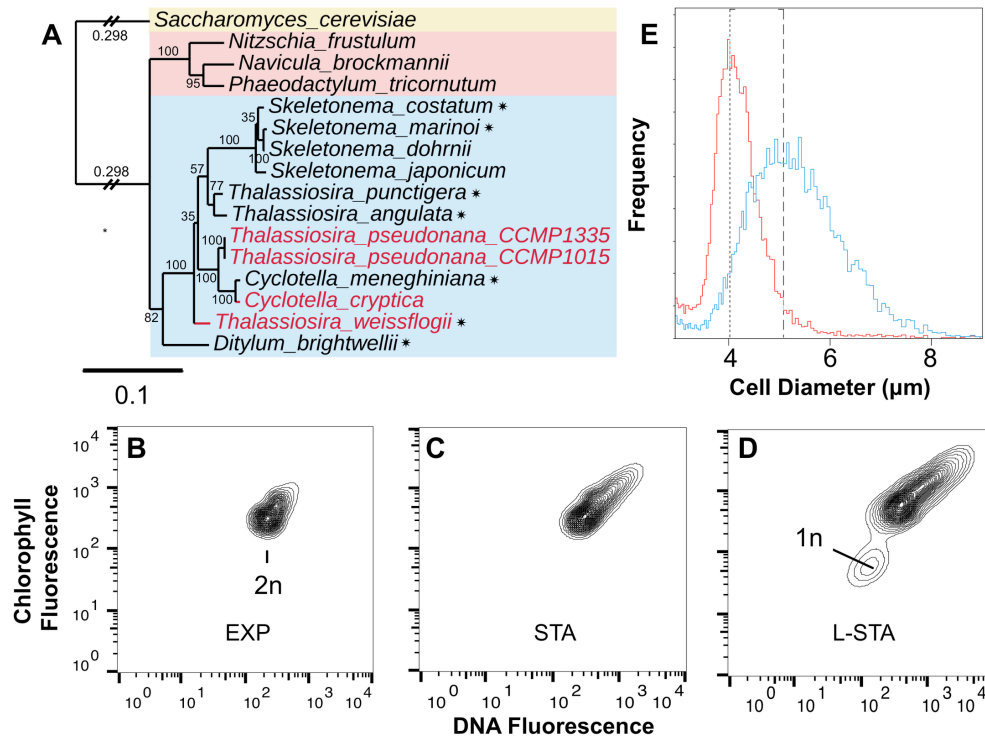


12  
 13 **Fig 2. Ammonium induces sexual morphologies in *T. pseudonana* CCMP1335. (A)**  
 14 Proportion of sexual cells (oogonia and auxospores) relative to the total population in cultures of  
 15 *T. pseudonana* grown in the presence of NH<sub>4</sub>Cl or NaNO<sub>3</sub>; n=3 independent cultures, average of  
 16 300 cells counted per replicate. Oogonia and auxospores were only observed beginning in  
 17 stationary phase, data are mean values, error bars are s.d.. Inset: corresponding growth curve  
 18 linking the onset of stationary phase with first appearance of sexual cells on day six. **(B)** Sexual  
 19 cells were observed in cultures with NH<sub>4</sub>Cl present at inoculation (blue hatched and solid blue  
 20 bars) or following NH<sub>4</sub>Cl addition at the onset of stationary phase (yellow bars). Legend shows  
 21 concentration of nitrogen source provided at inoculation and concentration of nitrogen source  
 22 added at the time of the second dosing. Two control treatments were supplied 200 μM nitrogen  
 23 source at inoculation only. Inset: corresponding growth curve showing the onset stationary phase  
 24 and timing of 2<sup>nd</sup> nitrogen addition; n=3 independent cultures, average of 281 cells counted per  
 25 replicate, data are mean values, error bars are s.d..  
 26



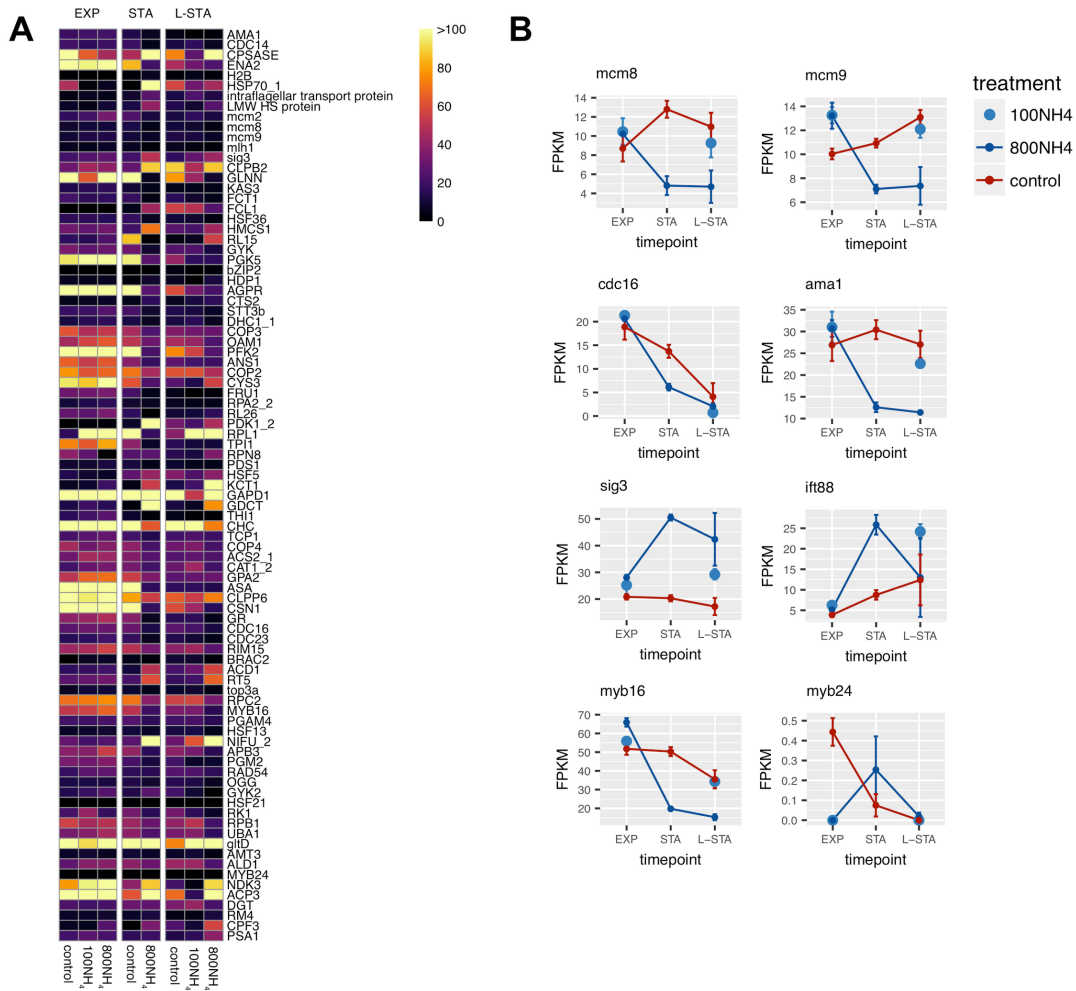
27  
28  
29  
30  
31  
32  
33  
34  
35  
36  
37  
38  
39  
40  
41  
42  
43  
44  
45  
46  
47  
48  
49  
50  
51  
52

**Fig 3. The life cycle stages of *T. pseudonana* (A-K), *T. weissflogii* (L) and *C. cryptica* (M-O) imaged using scanning electron microscopy (SEM), light (LM), and confocal microscopy (CFM). A:** Two vegetative cells (LM, CCMP1335). **B:** Oogonium displaying separation of thecae (arrowhead) and putative pycnotic nucleus indicated by the arrow (CFM, CCMP1015). **C:** Oogonium sharply bending at the thecae junction. Arrowhead indicates protrusion of the plasma membrane (CFM, CCMP1335). Oogonia images are representative of 38 total images. **D:** Spermatogonium containing multiple spermatocytes seen as individual red (DNA stained) clusters (CFM, CCMP1335); representative of 8 images. **E:** Motile spermatocytes (in red, arrow) with moving flagella (arrowheads, CFM, CCMP1335, representative of 10 images). **F-G:** SEM images of spermatocytes (arrowhead) attached to early oogonia (SEM, CCMP1335, representative of 20 images). **H,I:** Auxospores; representative of 60 images in CCMP1015 (H, LM) and CCMP1335 (I, CFM) showing bulging where mother valve was attached (arrowhead). Two nuclei are visible in red following non-cytokinetic mitosis. **J:** Small parental cell (arrow) with initial cells produced by sexual reproduction to the left (partial valve view) and right (girdle view) indicated by the arrowheads (SEM, CCMP1335). **K:** 7 x 12  $\mu\text{m}$  initial cell (LM); j and k representative of 12 images of CCMP1335. **L:** *T. weissflogii* auxospore (LM); representative of 12 similar images. **M:** *C. cryptica* spermatogonium (upper left) and vegetative cell (lower right). CFM shows stained DNA (red, arrow) and multiple nuclei in the spermatogonium. Arrowheads indicate chlorophyll autofluorescence (green). Oogonium (N, representative of 6 images) and auxospore (O, representative of 4 similar images) of *C. cryptica* (LM). Confocal microscopy images (b-e, i, m) show chlorophyll autofluorescence (green) and Hoescht 33342 stained DNA (red). Scale bars: A: 5  $\mu\text{m}$ ; B-E: 5  $\mu\text{m}$ ; F: 2  $\mu\text{m}$ ; G: 1  $\mu\text{m}$ ; H-O: 10  $\mu\text{m}$ .



53  
54  
55  
56  
57  
58  
59  
60  
61  
62  
63  
64  
65

**Fig 4. Evidence for meiosis and initial cells.** **A:** 18s rRNA phylogeny of diatoms including penates (pink rectangle), centrics (blue rectangle). Highlighted in red are the four strains induced into sexual reproduction in this study. Species for which some evidence already exists for sexual reproduction are starred [9, 13, 16, 28, 33, 38]. **B-D:** Changes in DNA and chlorophyll fluorescence in exponential (EXP), stationary (STA) and late stationary (L-STA) growth phases of *T. pseudonana* induced by ammonium; 30,000 events recorded, representative of two biological replicates. **E:** Coulter Counter distributions of cell diameter for *T. pseudonana* cultures in exponential phase of growth and maintained in NaNO<sub>3</sub> (red) and after six successive transfers to medium with ammonium (blue), single replicates of cultures with cell densities of 2.4 x 10<sup>6</sup> ml<sup>-1</sup> (NaNO<sub>3</sub>) and 2.3 x 10<sup>6</sup> ml<sup>-1</sup> (ammonium). Dashed lines are the mode for each peak.



66  
67  
68  
69  
70  
71  
72  
73  
74

**Fig 5. Transcriptomic evidence for sexual reproduction in *T. pseudonana*.** **A:** Heat map of 89 genes having annotated functions that were differentially expressed during differentiation and sexual reproduction in *T. pseudonana* CCMP1335. Color indicates normalized expression value (FPKM) for each nitrogen treatment (control = 100  $\mu\text{M}$   $\text{NO}_3^-$ ; 100NH4 = 100  $\mu\text{M}$   $\text{NH}_4^+$ ; 800NH4 = 800  $\mu\text{M}$   $\text{NH}_4^+$ ) and growth phase (EXP, STA, L-STA). **B:** FPKM values of select genes across growth phases for each nitrogen treatment.



75

76 **Supporting Information:**

77 **S1 Table. Pairwise comparison, Stationary phase 800  $\mu$ M Ammonium vs. exponential**

78 **phase 800  $\mu$ M Ammonium.**

79

80 **S2 Table. Pairwise comparison, Late-stationary phase 800  $\mu$ M Ammonium vs. exponential**

81 **phase 800  $\mu$ M Ammonium.**

82

83 **S3 Table. Pairwise comparison, Exponential phase 100  $\mu$ M Ammonium vs. Late stationary**

84 **phase 100  $\mu$ M Ammonium.**

85

86 **S4 Table. Pairwise comparison, Stationary phase 800  $\mu$ M Ammonium vs. Late stationary**

87 **phase 800  $\mu$ M Ammonium.**

88

89 **S5 Table. Pairwise comparison, Exponential phase nitrate vs. Exponential phase 800  $\mu$ M**

90 **Ammonium.**

91

92 **S6 Table. Pairwise comparison, Stationary phase nitrate vs. Stationary phase 800  $\mu$ M**

93 **Ammonium.**

94

95 **S7 Table. Pairwise comparison, Late Stationary phase nitrate vs. Late Stationary phase 800**

96  **$\mu$ M Ammonium.**

97

98 **S8 Table. Pairwise comparison, Exponential phase nitrate vs. Exponential phase 100  $\mu\text{M}$**   
99 **Ammonium.**  
100  
101 **S9 Table. Pairwise comparison, Late Stationary phase nitrate vs. Late Stationary phase 100**  
102  **$\mu\text{M}$  Ammonium.**  
103  
104 **S10 Table. Pairwise comparison, Exponential phase 100  $\mu\text{M}$  Ammonium vs. Exponential**  
105 **phase 800  $\mu\text{M}$  Ammonium.**  
106  
107 **S11 Table. Pairwise comparison, Late Stationary phase 100  $\mu\text{M}$  Ammonium vs. Late**  
108 **Stationary phase 800  $\mu\text{M}$  Ammonium.**  
109  
110 **S12 Table. Interaction analysis, Exponential - Stationary phases (800  $\mu\text{M}$  Ammonium v.**  
111 **Nitrate control).**  
112  
113 **S13 Table. Interaction analysis, Exponential - Late Stationary phases (800  $\mu\text{M}$  Ammonium**  
114 **v. Nitrate control).**  
115  
116 **S14 Table. Interaction analysis, Exponential - Late Stationary phases (100  $\mu\text{M}$  Ammonium**  
117 **v. Nitrate control).**  
118  
119 **S15 Table. Interaction analysis, Stationary - Late Stationary phases (800  $\mu\text{M}$  Ammonium v.**  
120 **Nitrate control).**

121

122 **S16 Table. Genes that were identified as differentially expressed in conditions that**  
123 **triggered cell differentiation and sexual reproduction and have annotated functions.**

124

125 **S17 Table. Genes that were identified as differentially expressed in conditions that**  
126 **triggered cell differentiation and sexual reproduction and are homologous to yeast genes**  
127 **involved in meiosis.**

128

129 **S18 Table. Genes that were identified as differentially expressed in conditions that**  
130 **triggered cell differentiation and sexual reproduction and are of red algal origin.**

131